Cite this article as: Tombak M., et al. (2025). The Interplay between Cellular Senescence and Side Population Stem Cells, *AgingBio*, *3*, e20250039. doi: 10.59368/agingbio.20250039.

Research Paper

The Interplay between Cellular Senescence and Side Population Stem Cells

Maria Tombak,[1] Anna Knyazer,[1] Ekaterina Rudnitsky,[1] Alex Braiman,[1] Orly Gershoni-Yahalom,[1] Benyamin Rosental,[1] Yael Segev,[1] Marina Wolfson,[1] Khachik K. Muradian,[2] Vera Gorbunova,[3] Gadi Turgeman[4] and Vadim E. Fraifeld[1,*]

[1]The Shraga Segal Department of Microbiology, Immunology and Genetics, Faculty of Health Sciences, Center for Multidisciplinary Research on Aging, Ben-Gurion University of the Negev, Beer-Sheva, Israel

[2]Department of Biology of Aging and Experimental Life Span Extension, State Institute of Gerontology of National Academy of Medical Sciences of Ukraine, Kiev, Ukraine

[3]Department of Biology, Rochester Aging Research Center, University of Rochester, Rochester, NY, USA

[4]Department of Molecular Biology, Faculty of Natural Sciences and Medical School, Ariel University, Ariel, Israel

[*]Corresponding author: vadim.fraifeld@gmail.com

Maria Tombak, Anna Knyazer, and Ekaterina Rudnitsky have equally contributed to this research.

https://doi.org/10.59368/agingbio.20250039

Received: 9/16/2024, Revised: 1/30/2025, Accepted: 2/16/2025, Published: 3/20/2025

Stemness and cellular senescence (CS) are fundamental and apparently opposite manifestations of cell plasticity. In the last years, evidence has been obtained indicating that pluripotency induced by Yamanaka's factors (OSKM) could promote CS, and *vice versa*. Whether the induction of cell reprogramming by defined small molecules (SMs) is also accompanied by acceleration of CS has not as yet been addressed. Side population (SP) stem cells have been found in all cell cultures and tissues examined thus far. The very existence of SP provides a natural model for investigating the links between CS and stem cells. However, the relationships between SP and CS, in particular the changes in SP abundance during the course of CS, have not yet been established. Here, we used primary cultures of human pulmonary fibroblasts (HPFs) to explore these relationships. The major findings of this study are: (a) biphasic changes in SP abundance during the course of CS, with a prominent increase in SP in pre-senescent HPF cultures followed by a dramatic decrease in the senescent stage; (b) SMs for cell reprogramming induce the accumulation of both SP stem cells and senescent cells, thus reminding the effects of Yamanaka's factors; (c) modifying CS by mesenchymal stem cell-derived extracellular vesicles coincided well with the dynamics of SP during the course of CS in HPF cultures and further strengthened the quantitative relationships between senescent and stem cells.

Introduction

Stemness and cellular senescence (CS) are fundamental and apparently opposite manifestations of cell plasticity. Recently, the evidence for the links between induced pluripotency and CS has been demonstrated (reviewed by ref.[1]). An unexpected finding was that the induction of pluripotency by defined Yamanaka's factors (OSKM: *Oct4*, *Sox2*, *Klf4*, and *c-Myc*) was accompanied by a massive accumulation of senescent cells, both *in vitro* and *in vivo*[2,3]. In turn, senescent cells supported induction of pluripotency and increased its efficacy[4]. In other words, cell reprogramming by defined factors could promote CS and *vice versa*. Moreover, CS was suggested to be an important or even obligatory component of cell reprogramming[2,3,5,6]. Yet, whether these relationships represent a "laboratory phenomenon" or reflect the fundamental physiological links are poorly investigated.

Side population (SP) cells were initially discovered by Goodell et al. (1996) as a distinct pool of cells with stem cell markers and an increased drug resistance[7]. Afterward, it has been proven that SP cells are stem cells which were found in each cell culture or tissue examined thus far[8–10]. The stem cell properties of SP have widely been recognized by their ability to differentiate into various cell types and express stem cell markers[9,11,12]. SP stem cells represent a very small but functionally meaningful cell pool, being involved in various physiological and pathological processes requiring tissue repair and regeneration[9,13]. Moreover, SP stem cells were recently included in clinical trials[14]. In a sense, SP could be considered a natural model allowing us to explore the interplay between stemness and CS. However, despite a broad scientific interest, this model has not yet been applied for studying the putative links between stem and senescent cells. Fibroblasts are a classical model for studying CS[15]. Also, fibroblasts (or, at least, their distinct subpopulation) are very similar or even indistinguishable from mesenchymal stem cells (MSCs) (reviewed by ref.[16]), which are considered as the main source of SP cells[17]. With this in mind, we used the primary cultures of human fibroblasts to explore the putative links between stem and senescent cells.

Materials and Methods

Cell culturing and counting

Primary cultures of human pulmonary fibroblasts (HPFs) (obtained from ScienCell Cat.#3300; Carlsbad, CA, USA) and

MCF-7 carcinoma (obtained from ATCC Cat.#HTB-22; Manassas, VA, USA) were grown under standard conditions (37 °C, 5% CO_2) in Dulbecco's modified Eagles medium (DMEM) (Cat.#01-055-1A), supplemented with 10% fetal bovine serum (Cat.#04-121-1A), 1% L-glutamine (Cat.#03-020-1B), and 1% penicillin/streptomycin (Cat.#03-031-5B). All products for cell cultures were from Biological Industries, Beit Haemek, Israel. The cultures were inspected daily under an inverted phase-contrast microscope (Primo Vert, Zeiss, Oberkochen, Germany), and cells were passaged 1:2 upon reaching 75%–80% confluence. The number and concentration of viable cells were calculated using the Trypan blue exclusion assay.

The model of replicative CS

CS was achieved by serial passaging. The cells were defined as pre-senescent or senescent, based on (a) a dramatic inhibition of cell proliferation or cell growth arrest, respectively; (b) typical CS morphology; and (c) expression of the CS markers, including senescence-associated β-galactosidase (SA-β-gal), the inhibitors of cell cycle $P16^{INK4a}$, $P21^{Cip1/Waf1}$, and senescence-associated secretory phenotype (SASP)-related *IL-6*.

SA-β-gal assay

The SA-β-gal assay was conducted on a six-well plate (50,000 cells per well) according to the manufacturer's protocol (Senescence Cells Histochemical Staining Kit Cat.#CS0030; Sigma-Aldrich, St. Louis, MO, USA). The cells were incubated with Staining Mixture for four hours at 37 °C. SA-β-gal staining was visualized using an inverted phase-contrast microscope (Primo Vert, Zeiss, Oberkochen, Germany).

mRNA isolation and quantitative real-time polymerase chain reaction (qRT-PCR)

RNA was extracted from cell pellets by the Blood/Cell Total RNA Mini Kit (Geneaid Cat.#RB300; New Taipei City, Taiwan), and 1 μg of total RNA was transcribed into cDNA in 20 μl reactions using the qScript cDNA Synthesis Kit (Agantek Cat.#95047; Yakum, Israel). qRT-PCR was performed using the SYBR Green Gene expression assays qPCRBIO SyGreen Blue Mix on the MIC 2 channel qRT-PCR system (Bio Molecular Systems; Upper Coomera, Australia), according to the manufacturer's instructions. In order to detect the expression of senescence-associated genes, multiple primer pairs were designed by the Primer-BLAST online tool and analyzed while the *GAPDH* or *PUM* gene was used as a normalization control (**Table S1**).

Fluorescence-activated cell sorting analysis and cell sorting

Fluorescence-activated cell sorting (FACS) was used to determine the presence and quantification of stem-like cells (SP) in the cultures of interest. The staining was carried out according to the established protocol[18,19], with minor modifications. For each SP analysis, 10^6 cells were resuspended in 1 ml of cell culture media DMEM supplemented with 2% FBS and 10 mmol/L of HEPES (pH 7.4; DMEM+). Cells were stained with 5 μg/ml Hoechst 33342 (Thermo Fisher Scientific Cat.#H3570, Waltham, MA) and incubated at 37 °C in a water bath for 90 min protected from light and mixed by vortexing every 20 min. To confirm the specificity of the SP signal, duplicate samples were incubated with calcium channel blocker and ABC blocker verapamil (Holland Moran Cat.#329330010, Yehud-Monosson, Israel) at a final concentration of 100 μM[20]. To assess viability, 7AAD (Biolegend Cat.#BLG-420403, San Diego, CA, USA) was added 30 min before the end of the incubation. The FACS analysis was performed using either Canto II or CytoFLEX systems, and the results were analyzed by FlowJo software V10. The intensity of Hoechst 33342 staining was measured in two channels—Ex. 405 nm, Em. 410–490 nm (Hoechst-Blue) and Ex. 405 nm, Em. 590–630 nm (Hoechst-Red). The cells were gated using the strategy illustrated in **Figure S1**. The gate for SP evaluation was selected based on verapamil treatment that served as a negative control (**Fig. S2**). Specifically, the SP gate included the area of the lowest fluorescence intensity in both Hoechst-Blue and Hoechst-Red channels, up to and excluding the dimmest verapamil-treated Hoechst-stained cells. The debris field characterized by Hoechst-Red high/Hoechst-Blue low fluorescence was also excluded. For cell sorting, $\sim 8 \times 10^6$ cells were collected, stained as described above, and sorted using an MA900 cell sorter (by Sony, Tokyo, Japan). Cell sorting was performed with a 100-μm nozzle size, and cells were sorted directly into 15 ml tubes containing 5 ml of DMEM + media in order to minimize cellular stress. Cells from SP and main population (MP) were sorted at a speed of 2500 cells/sec. Sorted SP and non-SP fractions were immediately seeded on six-well plates for further examination. For immunostaining with MSC or hematopoietic stem cell (HSC) markers, the cells defined as SP (i.e., stained with Hoechst 33242 as described above) were further incubated with the appropriate fluorescent antibodies (**Table S2**) following the manufacturers' recommended protocol.

Small molecule cocktail

The HPF cultures were treated with a cocktail containing small molecules (SMs) for cell reprogramming[21]: 0.5 mM valproic acid, 5 μM caffeic acid, and 10 μM LiCl (Cat.##1069-66-5, C-0625, and 7447-41-8, respectively; Sigma-Aldrich, St. Louis, MO, USA), 2 μM RepSox (BDL Beit Dekel Cat.#R0224-25MG, Raanana, Israel) (VCLR cocktail).

MSC-derived extracellular vesicles

Murine bone marrow-derived MSCs were isolated from ICR mice and characterized, as we previously described[22]. All experimental procedures were performed in accordance with National Institutes of Health guidelines. Extracellular vesicles (EVs) were isolated from conditioned media of MSC cultures at passages 13–15. Briefly, 70% confluent cultures were incubated with DMEM (low glucose) supplemented with 2 mM L-glutamine and 100 units/ml Penicillin and 100 mg/ml streptomycin for 48 hours. Conditioned media was centrifuged at 300*g* for 5 min to remove floating and dead cells, followed by additional centrifugation at 3000*g* for 10 min to remove debris. The supernatant was then ultracentrifuged at 100,000*g* for 70 min at 4 °C. The EV pellet was then resuspended in PBS and passed a second ultracentrifugation at 100,000*g* for 70 min at 4 °C. Isolated EVs were stored at −80 °C in PBS till use. EVs were characterized and quantified using Nanoparticle Tracking Analysis using NanoSight NS300 (Malvern Panalytical, Malvern, UK). EV size ranged mainly from 48 to 165 nm, and general morphology was confirmed by scanning electron microscopy. HPF cultures of pre-senescent (population doubling time [PDT] 6 days) or senescent (PDT > 3 weeks) stage were seeded in six-well plates and treated with 10^6 EVs per 1 ml of DMEM for 72 hours with one-week follow-up.

Statistical evaluation

The difference between experimental and control groups was evaluated using a two-tailed Student's t-test. P-values < 0.05 were considered statistically significant.

Results

Identification of SP cells in primary cultures of HPFs

To evaluate whether the primary cultures of HPFs contain stem cells, FACS analysis with the Hoechst dye was conducted. Because tumor cell cultures are known for their relatively high SP, we used MCF-7 human breast carcinoma cells as a positive control for the detection of stem cells. FACS analysis revealed a small population of verapamil-sensitive cells which excluded the Hoechst dye and a big population of the cells that did not exclude the Hoechst dye, both in normal HPF and MCF-7 carcinoma cell cultures (**Fig. S2**). According to Goodell et al.[7], verapamil-sensitive and verapamil-unsensitive cell pools represent SP of stem cells and MP of non-stem cells, respectively. In exponentially growing HPF cultures, the SP values vary from 0.03% to 0.15% (mean ± SE: 0.07 ± 0.02%; see **Fig. S2**). Of note, these values were particularly close to the percentage of SP cells reported for the total lung tissue (0.03%–0.07%)[23].

Cell sorting of HPF cultures for SP

Next, we examined the behavior of the SP and MP divided after cell sorting. The cells were grown in the DMEM medium optimized for fibroblast cultures. SP cells adhered rapidly to the flask surface, morphologically resembling the fibroblasts of early passages (long, thin spindle-like shape). Following three weeks of incubation, cell cultures derived from SP and MP were analyzed for their ability to efflux Hoechst dye (stemness phenotype). FACS analysis showed that in both cultures, the ratio of SP/MP tends to restore to the levels observed before cell sorting (**Fig. 1**). Thus, these observations indicate (a) the ability of SP stem cells to differentiate into mature fibroblasts, and (b) the ability of a small fraction of differentiated fibroblasts to undergo spontaneous cell reprogramming.

Sorted SP cells express mesenchymal but not HSC markers

Lung SP cells could be subdivided into two major subgroups: CD45-positive fraction with HSC potential and CD45-negative fraction with MSC phenotype[24]. To further evaluate the type of stem cells (hematopoietic or mesenchymal) present in HPF cultures, we analyzed the expression of corresponding markers in SP cells sorted by FACS. The FACS analysis with different markers revealed that SP cultures were negative for the HSC markers such as CD45, CD34, and CD133 (**Fig. 2A**). In contrast, the SP cells were positive for MSC markers including CD90, CD105, and CD44 (**Fig. 2B**). The results of FACS analysis were supported by qRT-PCR data on HPF cultures, which show that the expression of MSC markers is much higher in pre-senescent cell cultures (with a significantly higher SP fraction; see the next section) as compared to the young ones (**Fig. 2C**).

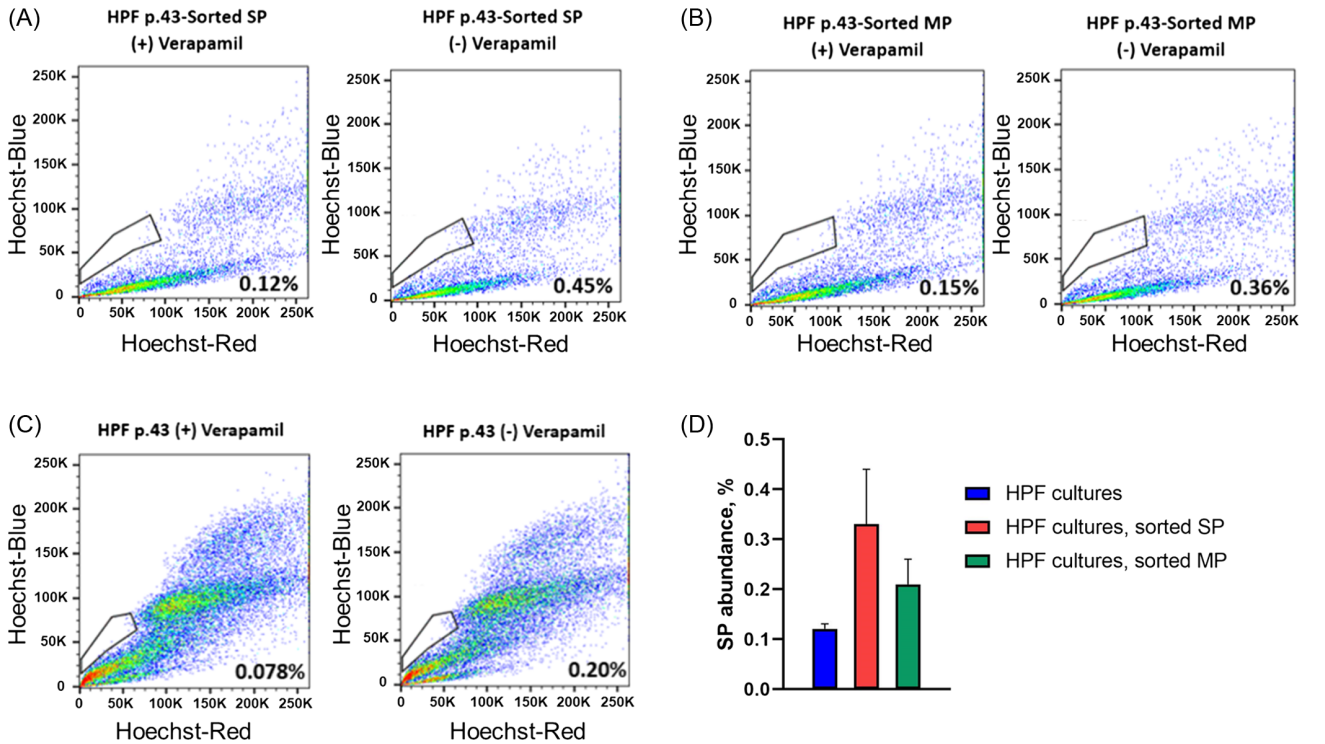

Figure 1. Sorted side population (SP)/main population (MP) cells restore their heterogeneity. Flow cytometry analysis of cultured cells: **(A)** three weeks after sorting human pulmonary fibroblast (HPF) cultures to SP cells; **(B)** three weeks after sorting HPF cultures to MP cells; and **(C)** control HPF cultures. Cell cultures were stained with Hoechst 33342 alone (−) or in combination with 50 μg/ml calcium channel blocker verapamil (+), as described in the Materials and Methods section. The percentage of SP cells was calculated as a difference between (−) verapamil and (+) verapamil. The gate for SP evaluation was selected based on verapamil treatment that served as a negative control (see also **Fig. S2**). **(D)** SP abundance in sorted and unsorted HPF cultures. The data are presented as mean ± SEM of at least three independent experiments.

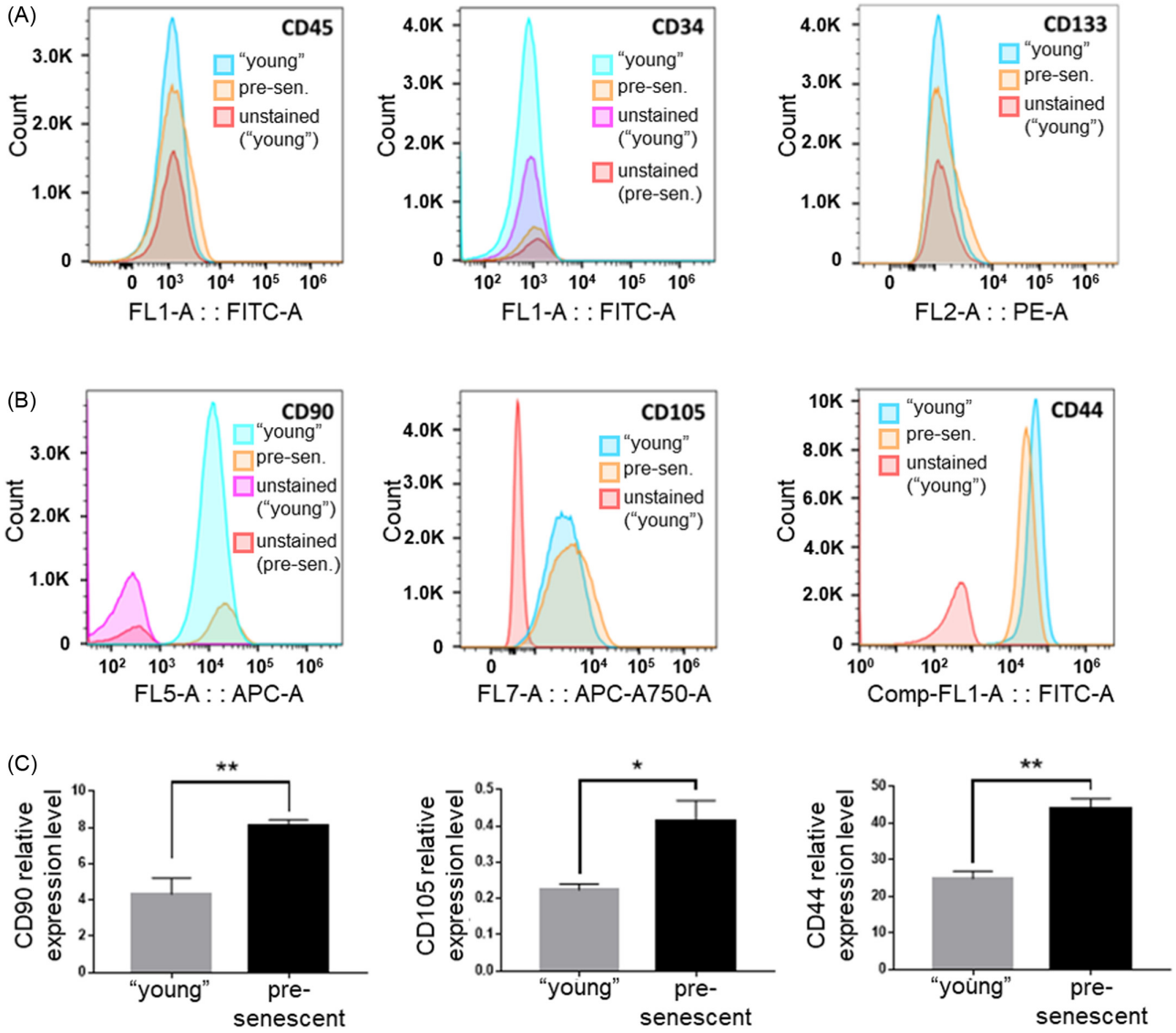

Figure 2. Expression of mesenchymal and hematopoietic markers in SP cells. Fibroblast cultures were analyzed by flow cytometry for SP cells with cell-surface expression of **(A)** mesenchymal CD90, CD105, CD44, or **(B)** hematopoietic CD45, CD34, CD133 stem cell markers. **(C)** RNA was extracted from HPF cultures; transcript levels of *THY1* (CD90), *ENG* (CD105), and *CD44* were determined by qRT-PCR and normalized to levels of the housekeeping gene *PUM*; values are the means of three independent experiments made in duplicates. "Young", HPF cultures of 17–20 passages; pre-senescent, HPF cultures of 40–45 passages. The data are presented as mean ± SEM. *$p < 0.05$; **$p < 0.01$.

Dynamics of SP during the course of replicative CS

The patterns of cell growth of primary cultures of HPFs, their morphology, and the expression of CS markers were similar to those described elsewhere (e.g., ref.[25]). The pulmonary fibroblasts of early passages (P.12–18, "young") displayed a typical spindle-like shape and doubled their population once a day. Approximately 20–25 passages later, the fibroblast cultures acquired more heterogeneous morphology with a small fraction of cells exhibiting SA-β-gal enzymatic activity and started to proliferate slower, and around passage 45–50 dramatically slowed down their growth (PDT 3–4 weeks) or ceased to divide (**Fig. 3A**). The fibroblast cultures of late passages had heterogeneous morphotypes, with large cells of irregular shape, and were stained with CS marker SA-β-gal (**Fig. 3B**). They expressed high levels of other CS markers, including the cyclin-dependent kinase inhibitors $P16^{INK4a}$, $P21^{Cip1/Waf1}$, and one of the main SASP components, *IL-6* (**Fig. 3C**).

We observed biphasic changes in SP during the course of replicative CS of human HPFs. As shown in **Figure 3D**, these changes in SP fraction occurred in a passage-dependent manner so that SP gradually increased with increasing passages and reached its maximum at the initial phase of CS (pre-senescent cultures). After that, SP decreased drastically, and in senescent cultures, fell down even below the level observed in "young" fibroblasts.

The effects of VCLR SM cocktail on SP and CS in primary cultures of HPFs

As mentioned above (see the Introduction section), the cell dedifferentiation induced by the defined transcription factors was accompanied by accumulation of senescent cells[2,3]. If these processes are also coupled after application of SMs for cell reprogramming has not yet been established. To clarify this point, we treated the HPF cultures with the SM cocktail (VCLR).

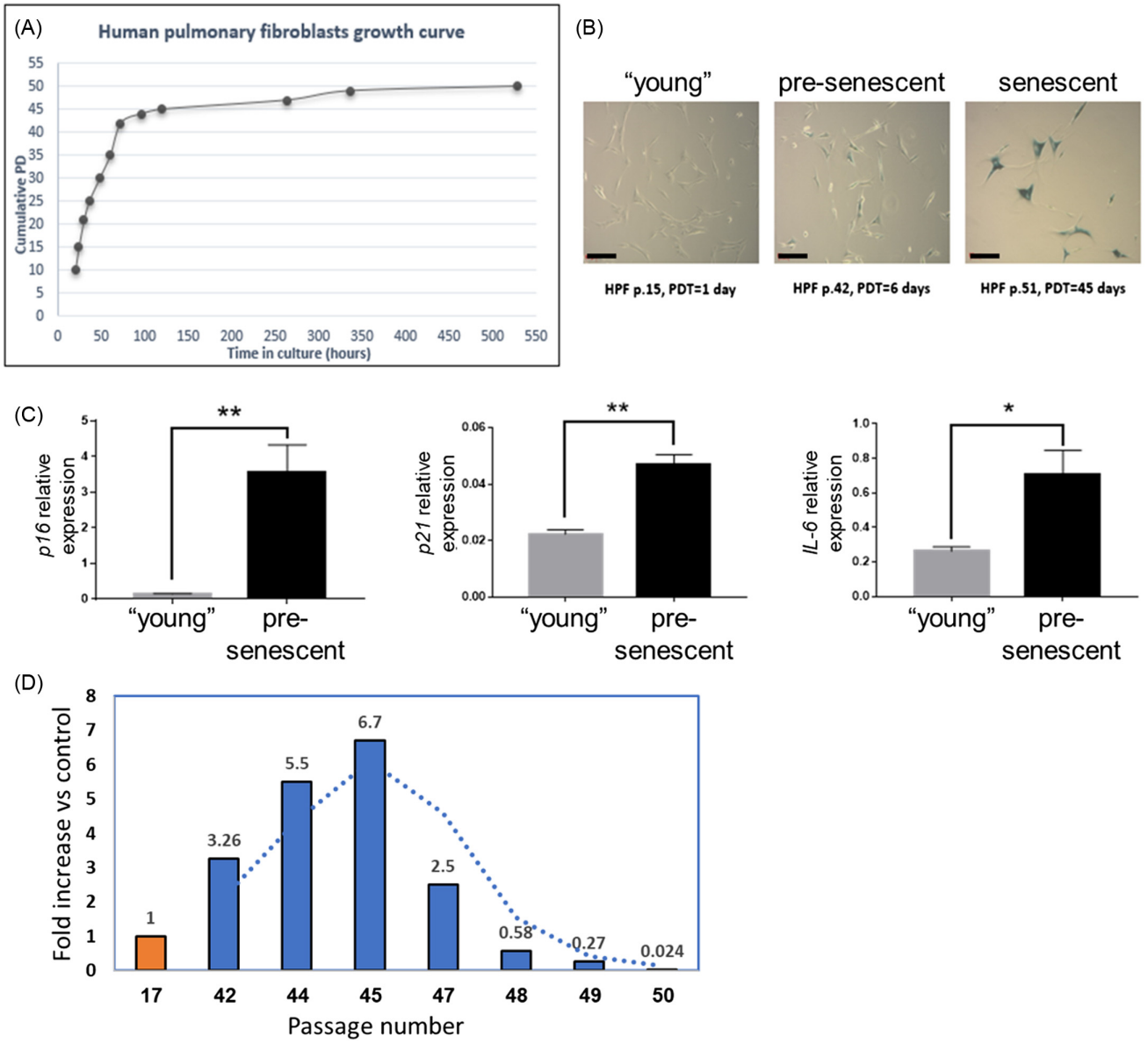

Figure 3. Primary HPF cultures in the course of cellular senescence (CS). (A) HPF growth curve; **(B)** senescence-associated β-galactosidase (SA-β-gal) staining of "young" (P.15), pre-senescent (P.42), and senescent (P.51) HPF cultures, the scale bar is 200 μm; **(C)** expression of CS-associated $P16^{INK4a}$ and $P21^{Cip1/Waf1}$ genes, and senescence-associated secretory phenotype (SASP)-related *IL-6* gene in "young" (p.15) and pre-senescent (p.42) HPF cultures. The data are presented as mean ± SEM. *$p < 0.05$; **$p < 0.01$. **(D)** Changes in SP abundance during the course of CS. In panels **(A)** and **(D)**, the means were calculated from several independent experiments ($n \geq 3$ for each point), and SEM is not presented for the sake of clarity.

The VCLR-treated cell cultures exhibited a significant increase in SP abundance versus control (untreated) HPF cultures, which peaked by six weeks of treatment (Fig. 4A).

As seen in Figure 3A, the primary cultures of the untreated HPFs did not show any slowing down of cell growth up to passage 40–45 and doubled their population once a day or two on average. In contrast, the VCLR-treated HPF cultures slowed down the cell growth (Fig. 4B) and began displaying alterations in cell morphology much earlier, starting from passage 18 to 19. As seen in Figure 4C, the HPF cultures of early passages (P.14), both the control and VCLR-treated, did not display any SA-β-gal enzymatic activity. The same picture is displayed in the control cultures till late passages. Yet, the opposite trend was observed in the VCLR-treated HPFs. After four weeks of incubation with the VCLR cocktail, many cells demonstrated positive staining for SA-β-gal, which peaked much earlier (P.29) than in control cultures. To further confirm accelerated CS in VCLR-treated HPFs, we examined the expression of $P21^{Cip1/Waf}$, $P16^{INK4a}$, and *IL-6* genes. As seen in Figure 4D, supplementation of the VCLR cocktail to HPFs resulted in an increased expression of all these CS markers. The results clearly demonstrated that the VCLR cocktail induced a premature CS of HPF cultures.

Effects of MSC-derived EVs on CS and SP abundance

A growing body of evidence indicates that MSC-derived EVs can affect CS[26]. Their effect on SP stem cells has not yet been

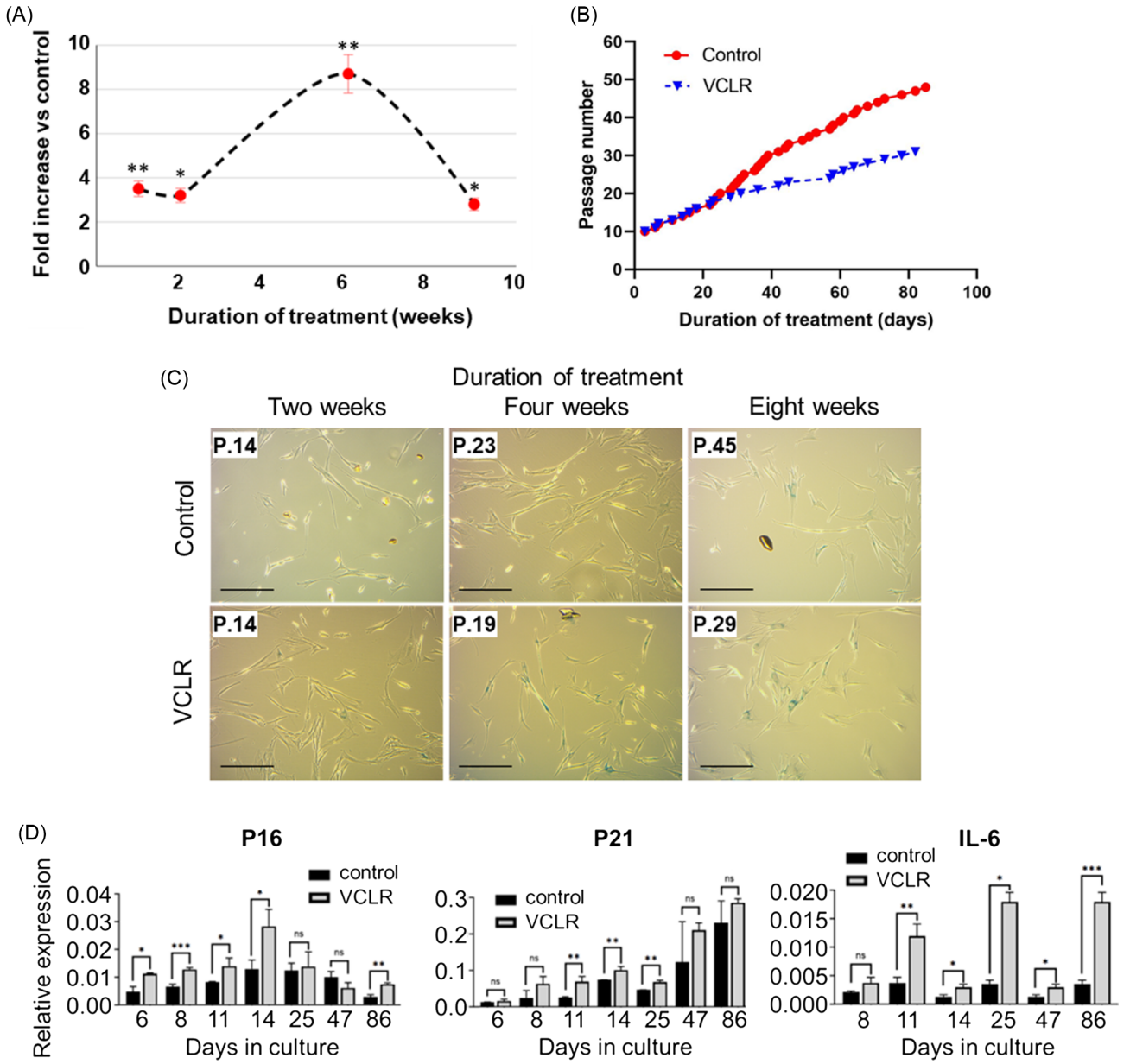

Figure 4. Effects of VCLR small molecule cocktail on primary cultures of HPFs. (A) The changes in SP cells in VCLR-treated cultures versus control; **(B)** cell growth curves for untreated and VCLR-treated HPF cultures; **(C)** SA-β-gal staining of untreated and VCLR-treated HPF cultures (Scale bar: 200 μm); **(D)** expression of CS-associated $P16^{INK4a}$ and $P21^{Cip1/Waf1}$ genes, and SASP-related *IL-6* gene in untreated and VCLR-treated HPF cultures. The data are presented as mean ± SEM. *treatment versus control, $p < 0.05$; **treatment versus control, $p < 0.01$; ***treatment versus control, $p < 0.001$.

established. With this in mind, we applied MSC-derived EVs to assess their impact on HPF cultures with regard to CS and SP. As seen in Figure 5A, the EV-treated HPF cultures of early pre-senescent stage (PDT 6 days) displayed a concomitant increase in both SP abundance and SA-β-gal-positive cells. An apparently inconsistent result was obtained in the EV-treated senescent HPF cultures (PDT ≥ 3 weeks). In this case, a clear trend ($p < 0.06$) for an increase in the percentage of SP stem cells was observed together with a significant decrease in the number of SA-β-gal-positive cells, which corresponds to the level of the late pre-senescent stage (Fig. 5B). On the whole, these findings coincide well with the dynamics of SP during the course of CS in HPF cultures (see Fig. 3D), pointing again to the quantitative relationships between senescent and stem cells.

Discussion

The existence of SP, a small pool of stem cells in cell cultures, provides a natural though still unexplored model for investigation of the relationships between senescent and stem cells. We used this model to shed light on the links between stemness and CS. For this purpose, we monitored the changes in SP abundance during the course of replicative CS and, on the other hand, applied cell reprogramming and/or CS-modifying agents. The major findings of this study include: (a) a prominent increase in SP in pre-senescent HPF cultures followed by a dramatic decrease in the senescent stage; (b) SMs for cell reprogramming induce the accumulation of both SP stem cells and senescent cells, thus reminding the effects of Yamanaka's factors;

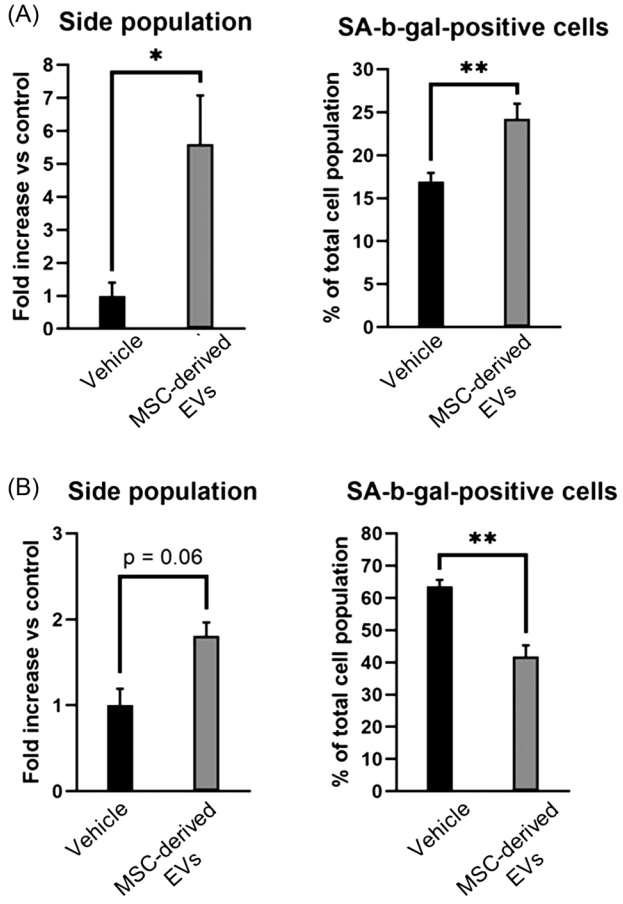

Figure 5. Effects of extracellular vesicles (EVs) on SP abundance and percentage of SA-β-gal-positive cells in HPF cultures. (A) Untreated and EV-treated pre-senescent HPF cultures (P.39). **(B)** Untreated and EV-treated senescent HPF cultures (P.51). The data are presented as mean ± SEM. *$p < 0.05$; **$p < 0.01$.

(c) modifying CS by MSC-derived EVs coincided well with the dynamics of SP during the course of CS in HPF cultures and further strengthened the quantitative relationships between senescent and stem cells.

Several lines of evidence indicated that CS can support the induction of pluripotency and increase its efficacy both *in vitro* and *in vivo* (reviewed by ref.[27]). It was suggested that this phenomenon is primarily attributed to IL-6 released by senescent cells[28,29]. Supplementation of IL-1β, IL-6, and/or TNFα to pancreatic β-cell or chondrocyte cultures further supported the role of SASP components in the promotion of somatic cell dedifferentiation[30,31]. At the same time, the CS-associated p53–p21 pathway is considered a barrier in the generation of iPSCs[32,33]. The same is true for *Ink4/Arf* locus containing $p16^{Ink4a}$, $p19^{Arf}$, and $p15^{Ink4b}$ genes: transient inhibition of this locus may significantly improve the generation of iPSCs[34,35]. The balance between *IL-6* and $P21^{Cip1/Waf1}/P16^{Ink4a}$ in HPFs during the course of CS may, to some extent, explain biphasic changes in SP abundance observed in this study. Indeed, the prevalence of *IL-6* in pre-senescent cultures led to an increase in SP percentage, while higher $P21^{Cip1/Waf1}/P16^{Ink4a}$ expression in senescent cultures resulted in a drop in SP (see **Fig. 2**). Interestingly, when an increase in senescent cells was not accompanied by an elevation in IL-6 expression, this was also accompanied by suppression of satellite cell expansion and muscle regeneration after injury[36]. Alternatively, cell damage and genotoxic stress, in particular, could promote both CS and an increase in SP. The concomitant accumulation of these two pools could occur because both senescent cells and stem cells are more resistant to apoptosis compared to actively dividing differentiated cells.

The increase in SP in pre-senescent HPF cultures could be attributed either to the proliferation of stem cells or to a dedifferentiation of cells from MP, or both. Our experiments on separate incubation of SP cells and MP cells after cell sorting of HPF cultures showed that the SP/MP ratio was restored in both sorted cultures. Indeed, following 3 weeks of incubation, the percentage of SP in both cultures reached the levels observed before cell sorting. Our results indicate the ability of SP cells to differentiate into the mature fibroblasts as well as the ability of mature fibroblasts from MP to dedifferentiate into SP, thus restoring the pool of stem cells. Putting in other words, we could suggest that a special regulatory loop keeps the balance between the mature and SP cells at a relatively constant level so that a certain fraction of mature cells permanently dedifferentiate into SP cells, and *vice versa*. The ability to preserve this balance could be a fundamental feature of any cell population, ensuring the maintenance of cell homeostasis.

Our *in vitro* observations appear to be functionally meaningful *in vivo* as well. Experiments on mice showed a large increase (over 25-fold) in SP cell frequency in aged mice compared to young ones. The authors also showed that SP cells in aged mice did not lose their stemness, albeit they had a lower homing efficiency than SP cells from younger mice[37]. Considering the age-related accumulation of senescent cells[38,39], it would be attractive to speculate that the increase in SP stem cells is a response to this accumulation, in order to maintain cellular homeostasis in tissues. From this point of view, it would be worth mentioning that the concentration of senescent cells in pre-senescent cultures is quite close to that in tissues of old animals[39].

As mentioned above, the induced pluripotency and cell reprogramming in general, achieved by the defined transcription factors (e.g., OSKM), are accompanied by the accumulation of senescent cells (reviewed by ref.[1]). Here, we expanded this important observation toward another inducer of cell dedifferentiation—SMs for cell reprogramming. Indeed, the VCLR-treated HPF cultures displayed the concomitant increase in the percentage of both SP cells and SA-β-gal-positive cells (see **Fig. 4**). Together with the data on Yamanaka's factors, it means that the elevation in the pools of dedifferentiated and senescent cells occurs independently of the nature of cell reprogramming inducers. Further supporting the relationships between senescent and stem cells are our observations on the effects of MSC-derived EVs (**Fig. 5**). These effects could differ between short- and long-lived species[40]. The links between CS and cell reprogramming are even more obvious when considering plant cells. Indeed, the dark-exposed *Nicotiana tabacum* leaves that underwent CS displayed characteristic features of dedifferentiating cells, including chromatin decondensation, disruption of the nucleolus, and condensation of rRNA genes[41,42]. It was suggested that cell dedifferentiation could be one of the outcomes of extreme stress conditions in mammals as well[43]. Altogether, these observations point toward deep relationships between opposing cell differentiation processes, cell reprogramming and CS, suggesting that interplay between them could be a general biological phenomenon.

Funding

This work was supported by the United States-Israel Research Foundation (BSF; grant number 2021287 to G.T., V.E.F., and V.G.). K.K.M. was awarded by Emergency Fellowships for Ukrainian researchers from The Israel Academy of Sciences and Humanities. E.R. was partially supported by the Israel Ministry of Aliyah and Integration.

Conflict of Interest

No conflict of interest is declared.

Supplementary Materials

Supplemental information can be found here: Supplementary.

References

1. Chiche A., Chen C., & Li H. (2020). The crosstalk between cellular reprogramming and senescence in aging and regeneration. *Exp. Gerontol.* **138**, 111005. PMID: 32561400; doi: 10.1016/j.exger.2020.111005.
2. Mosteiro L., Pantoja C., Alcazar N., Marión R.M., Chondronasiou D., Rovira M., … Gómez-López G. (2016). Tissue damage and senescence provide critical signals for cellular reprogramming in vivo. *Science* **354**(6315), 6315. PMID: 27884981; doi: 10.1126/science.aaf4445.
3. Mosteiro L., Pantoja C., de Martino A., & Serrano M. (2018). Senescence promotes in vivo reprogramming through $p16^{INK4a}$ and IL-6. *Aging Cell* **17**(2), e12711 . PMID: 29280266; doi: 10.1111/acel.12711.
4. Mahmoudi S. & Brunet A. (2012). Aging and reprogramming: A two-way street. *Curr. Opin. Cell Biol.* **24**(6), 744–756. PMID: 23146768; doi: 10.1016/j.ceb.2012.10.004.
5. Ritschka B., Storer M., Mas A., Heinzmann F., Ortells M.C., Morton J.P., … Keyes W.M. (2017). The senescence-associated secretory phenotype induces cellular plasticity and tissue regeneration. *Genes Dev.* **31**(2), 172–183. PMID: 28143833; doi: 10.1101/gad.290635.116.
6. Walters H.E., Troyanovskiy K.E., Graf A.M., & Yun M.H. (2023). Senescent cells enhance newt limb regeneration by promoting muscle dedifferentiation. *Aging Cell* **22**(6), e13826 . PMID: 37025070; doi: 10.1111/acel.13826.
7. Goodell M.A., Brose K., Paradis G., Conner A.S., & Mulligan R.C. (1996). Isolation and functional properties of murine hematopoietic stem cells that are replicating in vivo. *J. Exp. Med.* **183**(4), 1797–1806. PMID: 8666936; doi: 10.1084/jem.183.4.1797.
8. Asakura A. & Rudnicki M.A. (2002). Side population cells from diverse adult tissues are capable of in vitro hematopoietic differentiation. *Exp. Hematol.* **30**(11), 1339–1345. PMID: 12423688; doi: 10.1016/S0301-472X(02)00954-2.
9. Wolmarans E., Nel S., Durandt C., Mellet J., & Pepper M.S. (2018). Side population: Its use in the study of cellular heterogeneity and as a potential enrichment tool for rare cell populations. *Stem Cells Int.* **2018**, 1. PMID: 30627171; doi: 10.1155/2018/2472137.
10. Gamage T.K., Perry J.J., Fan V., Groom K., Chamley L.W., & James J.L. (2020). Side-population trophoblasts exhibit the differentiation potential of a trophoblast stem cell population, persist to term, and are reduced in fetal growth restriction. *Stem Cell Rev. Rep.* **16**(4), 764–775. PMID: 32548656; doi: 10.1007/s12015-020-09991-8.
11. Cervelló I., Gil-Sanchis C., Mas A., Delgado-Rosas F., Martínez-Conejero J.A., Galan A., … Horcajadas J.A. (2010). Human endometrial side population cells exhibit genotypic, phenotypic and functional features of somatic stem cells. *PLoS One* **5**(6), e10964 . PMID: 20585575; doi: 10.1371/journal.pone.0010964.
12. Wang F., Zhai X., Guo T., Xiao H., & Huang J. (2024). Effective detection of hoechst side population cells by flow cytometry. *J. Vis. Exp.* **210**, e67012 . PMID: 39248533; doi: 10.3791/67012.
13. Mimeault M. & Batra S.K. (2008). Recent progress on tissue-resident adult stem cell biology and their therapeutic implications. *Stem Cell Rev.* **4**(1), 27–49. PMID: 18288619; doi: 10.1007/s12015-008-9008-2.
14. Mohseni R., Hamidieh A.A., Shoae-Hassani A., Ghahvechi-Akbari M., Majma A., Mohammadi M., … Ashrafi M.R. (2022). An open-label phase 1 clinical trial of the allogeneic side population adipose-derived mesenchymal stem cells in SMA type 1 patients. *Neurol. Sci.* **43**(1), 399–410. PMID: 34032944; doi: 10.1007/s10072-021-05291-2.
15. Cristofalo V.J., Volker C., & Allen R.G. (2000). Use of the fibroblast model in the study of cellular senescence. *Methods Mol. Med.* **38**, 23–52. PMID: 22351263; doi: 10.1385/1-59259-070-5:23.
16. Soundararajan M. & Kannan S. (2018). Fibroblasts and mesenchymal stem cells: Two sides of the same coin? *J. Cell Physiol.* **233**(12), 9099–9109. PMID: 29943820; doi: 10.1002/jcp.26860.
17. Hu W., Ding R., Wang M., Huang P., Wei X., Hu X., & Hu T. (2023). Side population cells derived from hUCMSCs and hPMSCs could inhibit the malignant behaviors of Tn+ colorectal cancer cells from modifying their O-glycosylation status. *Stem Cell Res. Ther.* **14**(1), 145. PMID: 37237420; doi: 10.1186/s13287-023-03334-3.
18. Yin L., Castagnino P., & Assoian R.K. (2008). ABCG2 expression and side population abundancy regulated by a transforming growth factor beta-directed epithelial-mesenchymal transition. *Cancer Res.* **68**(3), 800–807. PMID: 18245481; doi: 10.1158/0008-5472.CAN-07-2545.
19. Golebiewska A., Brons N.H., Bjerkvig R., & Niclou S.P. (2011). Critical appraisal of the side population assay in stem cell and cancer stem cell research. *Cell Stem Cell* **8**(2), 136–147. PMID: 21295271; doi: 10.1016/j.stem.2011.01.007.
20. Shimoda M., Ota M., & Okada Y. (2018). Isolation of cancer stem cells by side population method. *Methods Mol. Biol.* **1692**, 49–59. PMID: 28986886; doi: 10.1007/978-1-4939-7401-6_5.
21. Knyazer A., Bunu G., Toren D., Mracica T.B., Segev Y., Wolfson M., … Fraifeld V.E. (2021). Small molecules for cell reprogramming: a systems biology analysis. *Aging (Albany NY)* **13**(24), 25739–25762. PMID: 34919532; doi: 10.18632/aging.203791.
22. Tfilin M., Gobshtis N., Fozailoff D., Fraifeld V.E., & Turgeman G. (2023). Polarized anti-inflammatory mesenchymal stem cells increase hippocampal neurogenesis and improve cognitive function in aged mice. *Int. J. Mol. Sci.* **24**(5), 4490. PMID: 36901920; doi: 10.3390/ijms24054490.
23. Summer R., Kotton D.N., Sun X., Ma B., Fitzsimmons K., & Fine A. (2003). Side population cells and Bcrp1 expression in lung. *Am. J. Physiol. Lung Cell Mol. Physiol.* **285**(1), L97–L104. PMID: 12626330; doi: 10.1152/ajplung.00009.2003.
24. Majka S.M., Beutz M.A., Hagen M., Izzo A.A., Voelkel N., & Helm K.M. (2005). Identification of novel resident pulmonary stem cells: Form and function of the lung side population. *Stem Cells* **23**(8), 1073–1081. PMID: 15987674; doi: 10.1634/stemcells.2005-0039.
25. Yehuda S., Yanai H., Priel E., & Fraifeld V.E. (2017). Differential decrease in soluble and DNA-bound telomerase in senescent human fibroblasts. *Biogerontology* **18**(4), 525–533. PMID: 28251405; doi: 10.1007/s10522-017-9688-6.
26. Rudnitsky E., Braiman A., Wolfson M., Muradian K.K., Gorbunova V., Turgeman G., & Fraifeld V.E. (2024). Stem cell-derived extracellular vesicles as senotherapeutics. *Ageing Res. Rev.* **99**, 102391. PMID: 38914266; doi: 10.1016/j.arr.2024.102391.
27. von Joest M., Chen C., Douché T., Chantrel J., Chiche A., Gianetto Q.G., … Li H. (2022). Amphiregulin mediates non-cell-autonomous effect of senescence on reprogramming. *Cell Rep.* **40**(2), 111074. PMID: 35830812; doi: 10.1016/j.celrep.2022.111074.
28. Chiche A. (2017). Injury-induced senescence enables in vivo reprogramming in skeletal muscle. *Cell Stem Cell* **20**(3), 407–414.e4. PMID: 28017795; doi: 10.1016/j.stem.2016.11.020.
29. Mahmoudi S., Mancini E., Xu L., Moore A., Jahanbani F., Hebestreit K., … Ang C.E. (2019). Heterogeneity in old fibroblasts is linked to variability in

reprogramming and wound healing. *Nature* **574**(7779), 553–558. PMID: 31645721; doi: 10.1038/s41586-019-1658-5.

30. Nordmann T.M., Dror E., Schulze F., Traub S., Berishvili E., Barbieux C., … Donath M.Y. (2017). The role of inflammation in β-cell dedifferentiation. *Sci. Rep.* **7**(1), 6285. PMID: 28740254; doi: 10.1038/s41598-017-06731-w.
31. Speichert S., Molotkov N., El Bagdadi K., Meurer A., Zaucke F., & Jenei-Lanzl Z. (2019). Role of norepinephrine in IL-1β-induced chondrocyte dedifferentiation under physioxia. *Int. J. Mol. Sci.* **20**(5), 1212. PMID: 30861996; doi: 10.3390/ijms20051212.
32. Hong H., Takahashi K., Ichisaka T., Aoi T., Kanagawa O., Nakagawa M., Okita K., & Yamanaka S. (2009). Suppression of induced pluripotent stem cell generation by the p53-p21 pathway. *Nature* **460**(7259), 1132–1135. PMID: 19668191; doi: 10.1038/nature08235.
33. Phanthong P., Raveh-Amit H., Li T., Kitiyanant Y., & Dinnyes A. (2013). Is aging a barrier to reprogramming? Lessons from induced pluripotent stem cells. *Biogerontology* **14**(6), 591–602. PMID: 23963527; doi: 10.1007/s10522-013-9455-2.
34. Li H., Collado M., Villasante A., Strati K., Ortega S., Cañamero M., … Serrano M. (2009). The Ink4/Arf locus is a barrier for iPS cell reprogramming. *Nature* **460**(7259), 1136–1139. PMID: 19668188; doi: 10.1038/nature08290.
35. Grafi G. (2013). Stress cycles in stem cells/iPSCs development: implications for tissue repair. *Biogerontology* **14**(6), 603–608. PMID: 23852045; doi: 10.1007/s10522-013-9445-4.
36. Moiseeva V., Cisneros A., Sica V., Deryagin O., Lai Y., Jung S., … Lukesova V. (2023). Senescence atlas reveals an aged-like inflamed niche that blunts muscle regeneration. *Nature* **613**(7942), 169–178. PMID: 36544018; doi: 10.1038/s41586-022-05535-x.
37. Pearce D.J., Anjos-Afonso F., Ridler C.M., Eddaoudi A., & Bonnet D. (2007). Age-dependent increase in side population distribution within hematopoiesis: implications for our understanding of the mechanism of aging. *Stem Cells* **25**(4), 828–835. PMID: 17158238; doi: 10.1634/stemcells.2006-0405.
38. Yanai H. & Fraifeld V.E. (2018). The role of cellular senescence in aging through the prism of Koch-like criteria. *Ageing Res. Rev.* **41**, 18–33. PMID: 29106993; doi: 10.1016/j.arr.2017.10.004.
39. Ogrodnik M. (2021). Cellular aging beyond cellular senescence: Markers of senescence prior to cell cycle arrest in vitro and in vivo. *Aging Cell* **20**(4), e13338 . PMID: 33711211; doi: 10.1111/acel.13338.
40. Emmrich S., Trapp A., Ganguly A., Biashad A.S., Ablaeva Y., Drage M.G., … Gorbunova V. (2024). Characterization of naked mole-rat mesenchymal stromal cells: Comparison with long- and short-lived mammals. *AgingBio* **2**(1), 20240029 . doi: 10.59368/agingbio.20240029.
41. Damri M., Granot G., Ben-Meir H., Avivi Y., Plaschkes I., Chalifa-Caspi V., … Fraifeld V. (2009). Senescing cells share common features with dedifferentiating cells. *Rejuvenation Res.* **12**(6), 435–443. PMID: 20041737; doi: 10.1089/rej.2009.0887.
42. Rapp Y.G., Ransbotyn V., & Grafi G. (2015). Senescence meets dedifferentiation. *Plants* **4**(3), 356–368. PMID: 27135333; doi: 10.3390/plants4030356.
43. Shoshani O. & Zipori D. (2011). Mammalian cell dedifferentiation as a possible outcome of stress. *Stem Cell Rev. Rep.* **7**(3), 488–493. PMID: 21279479; doi: 10.1007/s12015-011-9231-0.